SIMULATION OF A NOVEL EPROM STRUCTURE USING THE ENERGY-BALANCE EQUATIONS

Ph. Wolbert, E. van Schie, R. Wijburg, G. Hemink, J. Middelhoek
University of Twente, Faculty of Electrical Engineering
P.O. Box 217, 7500 AE Enschede, The Netherlands

Hot-carrier generation is not only considered to be a problem in modern MOSFET devices but could also be used beneficially in advanced device structures. Treatment of such hot-carrier phenomena necessitates the use of either time-consuming Monte-Carlo methods or the addition of the energy-balance equations to the DD-equations as in the hydrodynamic model [1].

In our 2D integrated process/device simulation program TRENDY [2] we have incorporated the HD model, using a discretization scheme for the energy-balance equations as proposed by Gnudi [3], while the current-continuity equations are discretized using a generalized Bernoulli approach [4]. The DD-equations and the energy-balance equations are solved alternately.

Fig. 1 shows a novel EPROM cell [5], using a buried injector. The electrons are accelerated perpendicular to the oxide-silicon interface, reaching their highest temperature just below the inversion layer. Some of the electrons will surmount the Si/SiO_2 barrier and will drift to the floating gate.

The EPROM has first been simulated using the process simulation part of TRENDY. First, the Monte-Carlo module has been used for the implantation process of source/drain and injector. Then, annealing and oxidation processes have been simulated to obtain the final doping profile. Half of the (symmetrical) device has been simulated with the device simulation part of TRENDY. Fig. 2 (log scale) shows the current density in injection mode (Vg=10V, Vd=5V), using the standard DD-model. Note the small hole current to the bulk contact, caused by avalanche generation just below the silicon-oxide interface, where the carrier energy is at its maximum.

In order to determine the electron temperature, the HD model was used with the hole temperature fixed at 300K. Fig. 3 again shows the simulated current density but now for the HD model. The current extends far deeper into the substrate than may be expected from the solution of the standard DD model. Fig 4 shows a 3D plot of the electron temperature multiplied by the electron current. Thus, filtering regions of less interest. Fig. 5 shows the electron temperatures for 2 different energy relaxation times at a cross-section in the middle of the device. No gate voltage is specified since the electron temperature is rather insensitive to it. From fig. 5 it can be seen that the maximum of the average(!) electron temperature lies just below the inversion layer. In the inversion layer itself, the temperature is low since there exists an excess of electrons (>1e20 cm-3).

We use Richardson's expression for the thermionic gate current, while the expression of Ning [6] is used for the effective barrier height. The electron concentration is taken at the top of the temperature peak to calculate the gate currents. In fig. 6, the measured and simulated injector and gate current are shown. The value of the gate current shows to be quite sensitive to the value of the relaxation time. Thus accurate quantitative results are difficult to obtain. The qualitative results are however promising enough to investigate how the EPROM can be optimized in future.

[1] A.Forghieri et al, IEEE Trans on CAD, vol. CAD-7, pp. 231-242, 1988.
[2] E.van Schie et al, *Software tools for process, device and circuit modeling,* Dublin: Boole, (W.Crans Ed.), pp. 155-161, 1989.
[3] A.Gnudi et al., SISDEP-3, (G. Baccarani Ed.), Bologna pp. 387-389, 1988.
[4] T.Tang, IEEE Trans. on Electron Devices, vol. ED-31, pp. 1912-1914, 1984.
[5] G.Hemink et al., ext. abstr of the 21st conf on SSDM, pp. 133-136, 1989.
[6] T.H. Ning et al., Journal of applied physics, vol. 48, pp. 286-293, 1977.

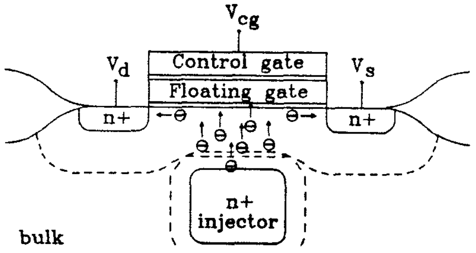

Fig 1: buried injector EPROM cell

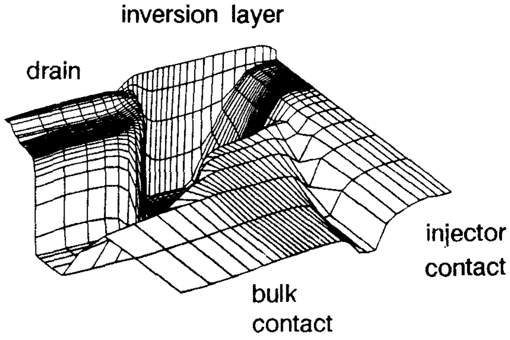

Fig 2: Log current density, DD model

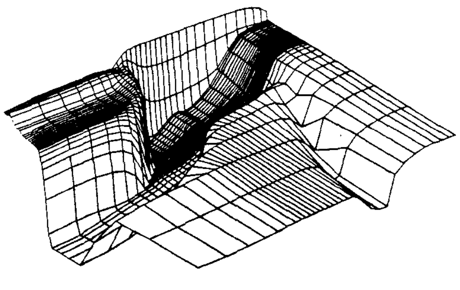

Fig 3: Log current density, HD model

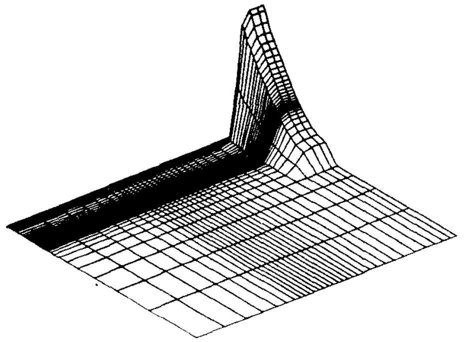

Fig 4: Electron temperature times JNY

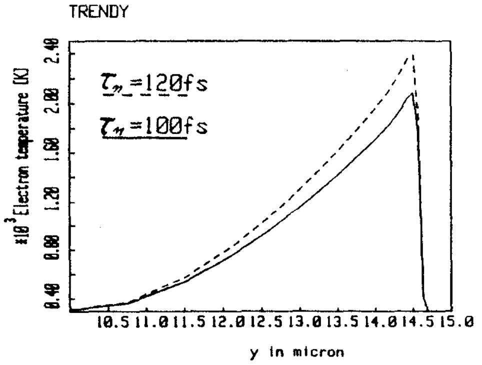

Fig 5: Electron temperature for $\tau_n = 100$ and $\tau_n = 120$ fsec

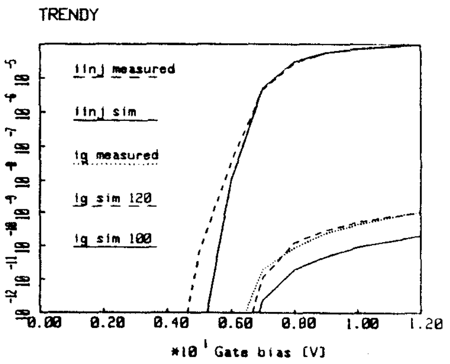

Fig 6: Measured and simulated characteristics